Carbohydrate Polymer Technologies and Applications 7 (2024) 100485

Contents lists available at ScienceDirect

Carbohydrate Polymer Technologies and Applications

journal homepage: www.sciencedirect.com/journal/carbohydrate-polymer-technologies-and-applications

# Gellan gum-based nanocomposites films containing bio-reduced silver nanoparticles: Synthesis, characterisation and antifungal activity

Laura Di Muzio [a], Francesco Cairone [a], Stefania Cesa [a], Claudia Sergi [b], Jacopo Tirillò [b], Letizia Angiolella [c], Andrea Giammarino [c], Gustavo Giusiano [d], Stefania Petralito [a], Maria Antonietta Casadei [a], Patrizia Paolicelli [a,*]

[a] Department of Drug Chemistry and Technologies, Sapienza University of Rome, 00185, Rome, Italy
[b] Department of Chemical Engineering Materials Environment, Sapienza University of Rome, 00184, Rome, Italy
[c] Department of Public Health and Infectious Diseases, Sapienza University of Rome, Rome, Italy
[d] Departamento de Micología, Instituto de Medicina Regional, Universidad Nacional del Nordeste, CONICET, Resistencia, Argentina

ARTICLE INFO

*Keywords:*
Film morphology
Silver nanoparticles
Low acyl gellan gum
Antifungal activity
Candida spp
Kiwi peels extract

ABSTRACT

The aim of this work was to develop and characterise nanocomposite thin films containing silver nanoparticles (AgNPs), as wound dressings and antifungal materials, using a green process for the nanoparticles' synthesis and a single step procedure for the preparation of the nanocomposite films. To this end, polyphenol-rich extracts obtained from kiwi peels, an agri-food industrial by-product, were used as a reducing agent of silver nitrate salt. The AgNPs were let form within the film-forming solution, which was composed by low acyl gellan gum and a plasticising agent (glycerol or PEG 400 g/mol) and the corresponding nanocomposite films were deposited by the solvent casting technique. The plasticising agent affected the AgNPs distribution within the films, as observed by SEM and EDS analyses, and consequently their tensile behaviour. In specific, AgNPs act as stress intensifiers in the presence of glycerol, whereas they act as film reinforcement with $PEG_{400}$. However, both glycerol-plasticised and $PEG_{400}$-plasticised films exhibited similar antifungal efficacy against 16 clinical isolates of 5 different Candida spp (*C. albicans, C. lusitaniae, C. haemulonii, C. krusei* and *C. glabrata*). Globally, the present study provides a green and single-step procedure to develop nanocomposite films embedding AgNPs obtained by *in situ* reduction of silver ions with polyphenol-rich extracts.

## 1. Introduction

Fungal infections, such as candidiasis caused by Candida, pose a problem of growing medical concern (Kainz, Bauer, Madeo & Carmona-Gutierrez, 2020). Furthermore, although the four most common Candida (*C. albicans, C. glabrata, C. parapsilosis*, and *C. tropicalis*) can account for more than 80 % of the cases, there is a long list of more than thirty Candida spp. that have been identified as candidemia agents (Gabaldón, Naranjo-Ortíz & Marcet-Houben, 2016). The emergence of resistant strains, including those becoming resistant to multiple drugs, has been increasingly reported in recent years (Pfaller, Diekema, Turnidge, Castanheira & Jones, 2019). This clinical issue is posing a demand for continuous research of effective medications. In this scenario, silver nanoparticles (AgNPs) deserve to be deepened for their promising antifungal activity (AlJindan & AlEraky, 2022; Perween, Khan & Fatima, 2019; Vazquez-Munoz, Lopez & Lopez-Ribot, 2020).

The antimicrobial activity of silver is known since long time. Despite this activity, it was abandoned with the discovery and diffusion of antibiotics and antifungal drugs (Paladini & Pollini, 2019). Over the last years, silver has made a comeback, and it has received significant attention because of the emergence of resistant strains and its low tendency to induce resistance. Therefore, it has been diffusing a renewing interest in silver use in wound care and there is consensus that topical silver treatment, in combination with good wound bed preparation, can help resolve wound infection. For this reason, different silver-containing dressings have been developed and commercialised for wound care management. These dressings can contain silver in different forms, however nanocomposite dressings having silver nanoparticles (AgNPs) inside are particularly beneficial for the treatment of infected wounds and burns (Khansa, Schoenbrunner, Kraft & Janis, 2019).

* Corresponding author at: Department of Drug Chemistry and Technologies, Sapienza University of Rome, Piazzale Aldo Moro 5, 00185, Rome.
*E-mail address:* patrizia.paolicelli@uniroma1.it (P. Paolicelli).

https://doi.org/10.1016/j.carpta.2024.100485

Available online 15 March 2024

Many techniques of AgNPs synthesis, such as chemical reduction of silver ions in aqueous solutions, have been reported in the literature. Most of these methods involve the use of toxic and hazardous chemicals, such as hydrazine or sodium borohydride, which may pose potential environmental and biological risks (Nie, Zhao & Xu, 2023). Therefore, the synthesis of metallic silver using these substances is unsustainable and carries risks related to the possibility of finding these substances, even in traces, in the final product. For this reason, there is a growing demand for environmental-friendly processes for AgNPs production that do not use toxic and polluting chemicals (Chen et al., 2021; Rahimi et al., 2020). One alternative and ecologically friendly approach for the synthesis of AgNPs is based on the use of plant extracts (Zuhrotun, Oktaviani & Hasanah, 2023). Different extracts derived from various parts of different plants, such as leaves, fruits, flowers, buds, pods, and so on, have been used as reducing agents in green synthesis processes to reduce metal silver ions to metal silver nanoparticles. The use of these natural extracts allows the reduction reaction to proceed slowly, and, in this way, they allow to achieve better control on the nucleation and aggregation of AgNPs. Indeed, an inverse relationship has been established between the formation rate of AgNPs and their size (Mogensen & Kneipp, 2014; Mukherji, Bharti, Shukla & Mukherji, 2019). Beside acting as reducing agents, these phytochemicals wrapped around the surface of AgNPs thus providing colloidal stabilisation to the synthesised AgNPs (Kanniah et al., 2021). Evidently, different natural extracts containing potentially reducing agents can be used for this purpose, however an approach that deserves consideration is based on the use and valorisation of agricultural wastes and industrial by-products to recover bioactive compounds (Chamorro et al., 2022). Based on these premises, the idea of the present study was a green synthesis of AgNPs by chemical reduction of a silver salt, using kiwi peels extracts, rich in polyphenols, as a reducing and capping agent. Extracts from kiwi fruit have already been used for the synthesis of AgNPs characterised by good antioxidant and antimicrobial activity (Bharathi et al., 2023; Mussin et al., 2021; Sun et al., 2021). Recently, Cairone et al. (2022) proposed an approach for the recycling and valorisation of kiwi peels, a waste by-product which contains high valuable bioactive molecules, such as polyphenols and antioxidants. The obtained kiwi peels hydroalcoholic extracts showed *in vitro* activity against *Candida albicans* and *Candida glabrata,* which may enhance the efficacy of AgNPs. Based on this premise, the present study investigates the use of these extracts for the bioreduction of silver ions and the preparation of nanocomposite films, containing AgNPs. Low acyl Gellan Gum (GG) was selected as film-forming polymer because of its non-toxicity, biocompatibility, and biodegradability (Priya et al., 2024). Despite these features and the well-known film-forming capacity, GG is one of the less investigated polymers for the development of nanocomposite films embedding AgNPs for biomedical purposes (Sheokand et al., 2023). The resulting films were characterised for the mechanical properties and the antifungal activity against different Candida spp. Nanocomposite films embedding AgNPs are generally evaluated for the antimicrobial properties, whereas their potential activity against yeasts has received only marginal attention and has been scarcely investigated, even though AgNPs have exhibited high antifungal activity against pathogenic Candida spp (Ahamad et al., 2022; AlJindan & AlEraky, 2022; Gibała et al., 2021; Vazquez-Munoz et al., 2020). For this reason, the present study dealt more specifically with the activity of silver nanocomposite films against clinical isolates of Candida spp. More specifically, the obtained nanocomposite films were tested *in vitro* against three strains of *Candida albicans,* four strains of *C. lusitaniae,* three strains of *C. haemulonii*, three strains of *C. krusei* and three strains of *C. glabrata*.

## 2. Materials and methods

### 2.1. Materials

Gellan gum (Gelzan), glycerol (Gly) and polyethylenglycole - PEG Mn 400 (380–420), PEG Mn 600 (570–630) and PEG Mn 4000 (3700–4400) were purchased from Sigma Aldrich. Silver nitrate ($AgNO_3$, > 99 %), monobasic potassium phosphate ($KH_2PO_4$, used to prepare phosphate buffer – PB – pH = 7.4), sodium hydroxide (NaOH) and hydrochloric acid (HCl) were purchased from Carlo Erba (Milan, Italy). Bidistilled water, anhydrous calcium chloride beads, acetone, ethanol, acetic acid, acetonitrile, isopropanol, hydrochloric acid 37 %, phosphate-buffered saline 1X (PBS) and formic acid were purchased from Merck life Science s.r.l (Milan, Italy). Reference compounds for HPLC analysis (gallic acid, alliin, (+)-catechin, chlorogenic acid, caffeic acid, epicatechin, *p*-coumaric acid, ferulic acid, sinapic acid, cyanidin-3-rutinoside, myricetin, quercetin, kaempferol) and 2,2-diphenyl-1-(2,4,6-trinitro-phenyl) hydrazine (DPPH) were purchased from Merck life Science s.r.l (Milan, Italy). Sabouraud Dextrose Agar (SDA) were purchased from Biolife, RPMI 1640 medium and 3-(N-morpholino)propanesulfonic acid buffer (MOPS) were obtained from Sigma Aldrich.

### 2.2. Kiwi peels extraction

Kiwi fruits (*Actinidia chinensis* L.) *cv*. Hayward, were collected manually from an organic plantation in Campania (Italy). The fruit epicarps were manually separated, dried and then submitted to hydroalcoholic extraction according to Cairone et al. (2022). About 25 g of dried peels were extracted with 75 mL of a hydroalcoholic mixture (ethanol:water acidified with 5 % of acetic acid, 70:30 *v/v*) for 3 h, at room temperature (25 °C), under stirring. The resulting final solution was filtered with qualitative Whatman® grade 1 filter paper (Merck Science Life s.r.l., Milan, Italy) and then concentrated under reduced pressure at 40 °C with a rotary evaporator (Laborota 4000, Heidolph), weighed and stored at 4 °C for maximum 24 h before analysis or use for film formulation.

### 2.3. Kiwi peels extract (PE) characterisation

#### 2.3.1. HPLC-DAD analysis

The extracts, dissolved in methanol, were analysed with a HPLC-DAD system (Perkin Elmer, Milan, Italy), equipped with a Series 200 LC pump, a Series 200 DAD and a Series 200 autosampler, including a TotalChrom Perkin Elmer software for plotting data. The analyses were performed on a Luna RP-18, 3 μm, with a linear gradient, constituted by acetonitrile and water acidified by 5 % formic acid, from 100 % of aqueous phase to 35 % in 55 min, at flow rate of 0.9 mL/min. Calibration curve was expressed in μg/mL and was constructed for catechin ($y = 5.18\ x - 24.29$; $R^2 = 0.9997$), (supplementary material, Figure S1 and Table S1).

#### 2.3.2. Evaluation of anti-radical activity by DPPH assay

The PE sample was submitted to anti-radical activity according to Cairone, Petralito, Scipione and Cesa (2021). 1 mL of extract solution (5 mg/mL isopropanol) was added to 2 mL of DPPH isopropanol solution 100 μM. The anti-radical activity was monitored using a UV/Vis Lambda 25 spectrophotometer Perkin Elmer (Waltham, MA, USA) and recorded at 515 nm. The activity was calculated using Eq. (1).

$$Inhibition\ \% = \frac{(Control\ Abs\ - Sample\ Abs)}{Control\ Abs} \times 100 \quad (1)$$

where Control Abs is the absorbance of the DPPH solution not containing PE, whereas Sample Abs is the absorbance of the DPPH solution containing PE. The antioxidant activity was expressed in mg equivalents of gallic acid/g extract (mg GA/g) as reported in Cairone et al. (2023).

### 2.4. AgNPs formation

AgNPs were formed following the reduction of $AgNO_3$ aqueous solutions induced by PE. To this end, aliquots of 0.5 % or 5.0 % *w/v* $AgNO_3$

solutions were mixed with opportune volumes of PE aqueous solution, achieving different $AgNO_3$:PE weight ratios (1:1; 1:2; 1:5; 1:10). More specifically, 1 mL of 0.5 % *w/v* of $AgNO_3$ solution was mixed with 83 μL, 166 μL, 415 μL or 830 μL of 60 mg/mL PE solution to give the different weight ratios (1:1; 1:2; 1:5; 1:10), then the total volume of the resulting solutions was raised to 2 mL. Similarly, 1 mL of 5.0 % *w/v* of $AgNO_3$ solution was mixed with 83 μL, 166 μL, 415 μL or 830 μL of 600 mg/mL PE solution to give the different weight ratios (1:1; 1:2; 1:5; 1:10), then the total volume of the resulting solutions was raised to 2 mL. All the solutions were maintained under magnetic stirring (250 rpm) wrapped with aluminium foil. The $Ag^+$ reduction reaction was carried out at 65.0 and 80.0 ± 0.5 °C for three different reaction times: 1, 3 and 5 h.

The effective $Ag^+$ reduction was evaluated by UV/Vis spectrophotometric analysis carried out with a Perkin-Elmer Lambda 40 spectrophotometer (Waltham, MA, USA). UV/Vis absorption spectra of silver nanoparticles were recorded at established time points, in the range 700–250 nm, at a resolution of 1 nm. Mixtures of PE and the plasticiser were used as blank. The AgNPs formation was also assessed by dynamic light scattering (DLS) analysis. A Zetasizer Nano-ZS DLS (Malvern Instruments, Worcestershire, UK) with a capability of measuring colloidal dispersions in the range of 0.3 nm–10 μm was used to determine the hydrodynamic diameter and polydispersity index (PDI) of the silver dispersions. The DLS technique used a photon correlator spectrometer equipped with a 4 mW He/Ne laser source operating at 633 nm. All measurements were performed at a scattering angle of 90° and were thermostatically controlled at 25 °C. The samples were opportunely diluted with demineralised water before analysis in order to avoid multiple scattering effects.

### 2.5. Rheological characterisation of the film-forming solutions

The rheological measurements were conducted using a Discovery TA HR-1 stress control rheometer (TA Instruments, New Castle, DE, USA). A cone-plate geometry with a diameter of 40 mm ($\alpha$ 1.005°, gap 27 μm) was used for all the analyses. Solutions of GG and different plasticising agents, namely Gly, $PEG_{400}$, $PEG_{600}$ and $PEG_{4000}$, were prepared, solubilising both the components, at a concentration of 2.0 % *w/v*, in distilled water at 80 ± 1 °C for 3 h under magnetic stirring. Then, 0.5 mL of the obtained solutions were poured on the pre-heated Peltier plate of the rheometer. Oscillatory temperature-sweep analyses were carried out by decreasing the temperature at a rate of 3.0 ± 0.1 °C/min, keeping a constant frequency of 1 Hz and a deformation of 1 %, which was determined with previous oscillatory strain-sweep tests. Temperature sweep analyses were also carried out on film-forming solutions containing the PE (0.05 % *w/v*). In addition, flow-sweep measurements were carried out on GG solutions (2.0 % *w/v*) containing or not containing the plasticiser (Gly or $PEG_{400}$, 2.0 % *w/v*) and the PE (0.05 % *w/v*). In particular, the viscosity as a function of the shear rate was measured, applying shear stresses in the range of 0.5–700 Pa. The flow-sweep measurements were carried out at 65.0 ± 0.1 °C, the same temperature employed during the casting process. All the experiments were carried out at least in triplicate.

### 2.6. Film preparation

GG-based films were produced using the solvent casting technique (Paolicelli et al., 2018) following two different procedures. In both cases, nanocomposite films were obtained casting 6 mL of the film-forming solutions prepared in distilled water and containing the AgNPs. The first procedure involves the initial formation of the AgNPs followed by the addition of GG. More specifically, 150 μL of 20 mg/mL $AgNO_3$ aqueous solution and 50 μL of 60 mg/mL PE aqueous solution were added to 5.8 mL of an aqueous solution of Gly or PEG to give a final concentration of the plasticising agent of 2 % *w/v*. The obtained solutions were maintained under magnetic stirring (250 rpm) at 65.0 ± 0.5 °C for 3 h to allow the AgNPs formation. After this time, 0.12 g GG was added to the dispersion to have a 2 % *w/v* polymer concentration and the mixture was stirred (100 rpm) at 65.0 ± 0.5 °C for 2 h. After complete polymer dissolution, the mixtures were poured onto levelled silicone baking moulds (diameter 5.6 cm), and oven-dried at the constant temperature of 40 ± 2 °C for 15 h. Following this procedure, two different films were obtained, which were labelled F1-Gly and F1-PEG. According to the second procedure, instead, 0.12 g of both GG and the plasticiser (Gly or PEG) were dissolved in 5.8 mL of distilled water at 80 °C for 2 h under magnetic stirring (250 rpm). After complete dissolution, the temperature was decreased to 65.0 ± 0.5 °C and then 150 μL of 20 mg/mL $AgNO_3$ aqueous solution and 50 μL of 60 mg/mL PE aqueous solution were added. Both GG and the plasticising agent had a concentration of 2 % *w/v* in the film-forming solution. The polymeric mixtures were maintained at 65.0 ± 0.5 °C for 1 h under magnetic stirring (250 rpm), then the mixtures were stirred at 100 rpm for further 2 h to allow the AgNPs formation, while avoiding air bubbles. After this time, the mixtures were poured onto levelled silicone moulds (diameter 5.6 cm), and oven-dried at the constant temperature of 40 ± 2 °C for 15 h. Following this procedure, two different films were obtained, which were labelled F2-Gly and F2-PEG. The second protocol was also used to prepare films with higher silver content. In the specific, 300 μL of 20 mg/mL $AgNO_3$ aqueous solution and 100 μL of 60 mg/mL PE aqueous solution were added to 5.6 mL of previously prepared GG/plasticiser solutions. Also in this case, both GG and the plasticising agent had a concentration of 2 % *w/v*. The mixtures were maintained for 1 h at 65.0 ± 0.5 °C under magnetic stirring (250 rpm), then the mixtures were stirred at 100 rpm for further 2 h to allow the AgNPs formation, while avoiding air bubbles. Then the mixtures were casted onto levelled silicone baking moulds (diameter 5.6 cm), and oven-dried at the constant temperature of 40 ± 2 °C for 15 h. The obtained films were labelled F3-Gly and F3-PEG. Finally, under the same experimental conditions, plain films, which did not contain AgNPs, were prepared and used as a control. These control films were labelled F0-Gly and F0-PEG.

### 2.7. Film characterisation

Films were characterised for their physical and mechanical properties as described in the following sections.

#### 2.7.1. Measurement of film thickness and density

The thickness of all the prepared films was measured by using the thickness gauge Mitutoyo Digimatic Micrometer. The measurements were carried out in six different points of the same film in order to evaluate the homogeneity of the prepared samples.

For density evaluation, circular specimens were cut with a biopsy punch (diameter 8 mm) and weighed. Density was expressed as $g/cm^3$ and determined at least 3 times with different samples of each film formulation.

The results of thickness and density were reported as mean values ± standard deviation.

#### 2.7.2. Colour and optical transparency measurements

Colorimetric analysis of the nanocomposite GG-based films was carried out using a MetaVue X-rite TM colorimeter, featuring a LED illuminant/45–0°. The $L^*$, $a^*$, $b^*$, $C^*_{ab}$, $h^\circ$ values were calculated using the iColor software. The CIEL*a*b* parameters were used to describe the chromatic properties of the different film formulations.

Optical transparency of the nanocomposite GG-based films was evaluated measuring light transmittance at 650 nm with a Perkin-Elmer Lambda 40 spectrophotometer (Waltham, MA, USA).

#### 2.7.3. Scanning electron microscopy (SEM) and energy dispersive spectroscopy (EDS)

Films were morphologically characterised through a field-emission scanning electron microscope (FE-SEM) MIRA 3 by Tescan. Films were applied on a sample holder by using a conductive adhesive to prevent

charging. A beam voltage of 10.0 kV and a working distance of 15 mm were used. The morphological characterisation was supported by an elemental analysis through the EDS Octane Elect by Edax.

#### 2.7.4. Mechanical characterisation: tensile tests

The mechanical performance of the films was evaluated through tensile testing performed with a Zwick/Roell Z010 equipped with a 1000 N load cell. A test speed of 2 mm/min and a grip-to-grip separation of 15 mm were used. At least four samples for each different film were tested and the results were reported as mean values ± standard deviation.

#### 2.7.5. Water vapour permeability (WVP)

The measurements of the WVP were carried out gravimetrically as described by Huang, Maltais and Wang (2023). Circular film samples were mounted on the open mouth of cylindrical plastic cups containing a weighed quantity of anhydrous calcium chloride (0 % relative humidity, RH). The sealed cylindrical cups were placed inside a desiccator containing water (100 % RH) and all the assemblies were then maintained at 32 °C in an incubator. After 24 h, the weight change of the cups was recorded and used to calculate the WVP (g $m^{-1}$ $h^{-1}$ $Pa^{-1}$) by Eq. (2).

$$WVP = \frac{\Delta m \times k}{A \times \Delta t \times \Delta P} \quad (2)$$

where $\Delta m$ is the weight change of the cup during time $t$, $k$ is the thickness of the film, $A$ is the exposed area of the film, and $\Delta P$ is the partial water vapor pressure difference between two sides of the film.

### 2.8. Swelling studies

The nanocomposite films were characterised through dynamic swelling measurements. Each film was divided into parts of comparable size, weighed and immersed in 15 mL of PB (pH = 7.4) or PBS (pH = 7.4) at 37.0 ± 1.0 °C. At predetermined time points, the samples were extracted from the medium, gently wiped to remove the liquid in excess and weighed. The degree of swelling ($Q$) was calculated using Eq. (3).

$$Q = \frac{W_s}{W_d} \quad (3)$$

where $W_s$ and $W_d$ represent respectively the weight of the swollen sample at time $t$ and that of the dry sample. The measurements were continued up to 5 h.

The experiments were carried out at least in triplicate and the results were reported as mean values ± standard deviation.

### 2.9. Antifungal activity of films loaded with AgNPs

In this study three vaginal isolates of *C. albicans* (IMR 1462, IMR1463 and IMR1464), four *C. lusitaniae* (IMR301, IMR1112 isolated from blood and IMR522, IMR1384 isolated from urine), three blood isolates of *C. haemulonii* (IMR 785, IMR1293 and IMR1375), three *C. glabrata* (1511, 43,976, isolated from blood and IMR1099 reference strain) and three *C. krusei* (IMR1465 laboratory strain, 45,709, and 44,956 isolated from urine) were studied. All isolates were identified by MALDI-TOF and deposited in the culture collection (IMR-M) of the Mycology Department, Instituto de Medicina Regional, Universidad Nacional del Nordeste (Argentina). All strains were maintained in Sabouraud Dextrose (SD) Agar.

For the antifungal activity $2 \times 10^3$ cells/mL were grown on circular samples (diameter 8 mm) of plain films (F0-Gly and F0-PEG) and nanocomposite films containing AgNPs (F2-Gly, F2-PEG, F3-Gly and F3-PEG) in 24-well plates containing 1 mL of RPMI 1640 medium supplemented with 3-(N-morpholino)propanesulfonic acid buffer (MOPS). The plates were incubated at 28 °C for 24 h and 48 h. Then incubation for 24 h and 48 h, 10 μL of the medium from each well, was spread on plates containing Sabouraud Dextrose Agar (SDA) and incubated for 24 h at 28 °C for colony count determination (CFU). Each experiment was repeated three times.

### 2.10. Statistical analysis

Inferential statistic was used to determine if the film type and the Ag content met the criteria for statistical significance proving to have an actual effect on the dependent variable, *i.e.* tensile modulus and strength. In particular, the *F*-test (ANOVA) was used for the analysis and a $p$-value $< 0.05$ or lower was adopted as statistically significant limit, thus meaning that a $p$-value lower than 0.05 confirms that the parameter under consideration had an actual effect on the dependent variable. The analysis was carried out with the R-studio software applying a linear model (lm) which accounts also for film type and Ag content interaction. The same analysis was also used for swelling data.

Statistical differences among the groups of data related to the antifungal activity were analysed by one-way ANOVA with Sidak's post hoc test. In all the comparisons, a $p$-value of 0.05 or lower was considered significant. The analyses were done in the software Graph pad prism Software version 8.0.1.

## 3. Results and discussion

### 3.1. Polyphenols extraction and characterisation

As known, polyphenols, and in particular flavonoids, are a class of molecules with excellent antioxidant and anti-radical activity, due to the presence of hydroxyl and even catechol groups in resonance with the aromatic rings, characterising this class of compounds (Stagos, 2019).

The polyphenolic profile of kiwifruit is mainly characterised by compounds such as benzoic and hydroxycinnamic acids, which are particularly concentrated in the peels. The most common compounds are flavanols (catechins and epicatechins), protocatechuic acid, ferulic acid, caffeic acid, hydroxybenzoic acid, and coumaric acid (Cairone et al., 2022; Deng et al., 2016; Dias et al., 2020).

Industrial processing of fruits and vegetables generates a large amount of waste and these by-products could be managed and utilised more efficiently. These by-products are, in fact, rich in bioactive components from different fruit seeds and peels. By-products from the food and cosmetic industries are now considered as new sources of polyphenolic compounds, and therefore the effective utilisation of these waste materials has recently generated increasing interest among scientists (Gil-Martín et al., 2022; Reguengo, Salgaço, Sivieri & Marostica Júnior, 2022).

In view of these considerations, a hydroalcoholic extraction, performed on separated peels of kiwi fruits, allowed us to obtain PE samples highly enriched in polyphenols, thus valorising an agricultural by-product of the industrial kiwifruit juice supply chain (Cairone et al., 2022). The obtained PE samples were then used for the biogenic synthesis of AgNPs. The AgNPs production starting from biological materials, such as plant leaves, stems, roots, and flowers, is nowadays preferred due to their eco-friendly nature, cost-effectiveness, and less involvement of toxic chemicals (Rodríguez-Félix et al., 2021; Salayová et al., 2021). With five hundred tons of AgNPs produced per year, silver-based nanomaterials represent one of the most commercialised systems, which is expected to increase in the next few years (Tyagi et al., 2021). Therefore, the development of environmentally friendly methods for the synthesis of AgNPs has become a hot topic in recent years and, among them, the biogenic approach is worthy of consideration (Vanlalveni et al., 2021).

#### 3.1.1. HPLC-DAD analysis and DPPH assay

Previously, our research group had developed nanocomposite films containing AgNPs, obtained by photoreduction of silver ions (Di Muzio et al., 2022). In this work, it was evaluated the feasibility of a mild

bioreduction of silver ions into AgNPs to be included within GG-based film dressings. The PE sample, to be used at this end, was analysed with a HPLC-DAD method, recording data at 280 nm (supplementary material, Figure S2). The obtained chromatogram showed a quite simple profile characterised by only four principal peaks. These were presumably ascribable to ascorbic acid ($t_r$ = 3.95 min), a catechin derivative ($t_r$ = 9.73 min), a cinnamic acid derivative ($t_r$ = 38.71) and a terpene derivative ($t_r$ = 48.14 min). Qualitative identification of the signals observed at 280 nm was performed by comparison with the literature (Liu et al., 2022; Zhang et al., 2021). Since only catechin could be identified by external commercial standard, the polyphenol fraction was, in the whole, quantified as the sum of the peak areas recorded at 280 nm and expressed as catechin equivalents. The found values, of about 16 mg/g of extract, result in line with previous data obtained by our group (Cairone et al., 2022) and other research groups (Aires & Carvalho, 2020; Silva et al., 2023), that found amounts of total polyphenols (TPC assay) between 0.6 and 20 mg/g of extract. As reported in some papers (Onitsuka, Hamada & Okamura, 2019; Rolim et al., 2019), catechins found in black and green tea were able, not only to reduce silver ions, but also to stabilise the resulting AgNPs, acting as capping agents. The presence of flavanols derivatives, together with a residual content of reducing sugars and ascorbic acid, could be of crucial importance in assisting the reduction of silver ions. Further studies could be of interest to investigate the fingerprint of different PE samples to be employed with this aim.

The antioxidant power of PE was also evaluated by DPPH spectrophotometric assay. Analyses showed an antioxidant activity between 45 and 50 % inhibition. These results were also expressed as mg equivalents of gallic acid/g extract (mg GA/g) (Cairone et al., 2023) giving values in the range 6–8 mg GA/g. Previous studies (Cairone et al., 2022; Hădărugă, Pantea & Hădărugă, 2016) reported scattered results (22–80 % inhibition) according to the hydroalcoholic composition, which in turn could depend on the cultivar and the geographical area, with values rising with increasing ethanol percentage used for the extraction process. Our data highlight good antioxidant activity of the obtained extracts, with promising outcomes for the nanocomposite films formulation. Indeed, the use of the polyphenolic extracts obtained from kiwifruit peels, allows not only to valorise a by-product of the agricultural supply chain, but also to reduce $Ag^+$ ions to $Ag^0$ and promote the formation of AgNPs through a green process, that allows avoiding the use of aggressive and toxic reducing agents (Malik et al., 2022).

### 3.2. Film preparation and optimisation

The procedure used to obtain nanocomposite GG-based films containing AgNPs was developed considering previous works (Adrover et al., 2020; Paolicelli et al., 2018), but also the experimental conditions required for the formation of AgNPs. Indeed, the procedure for the film fabrication was opportunely optimised to allow the *in situ* synthesis of the AgNPs into the filmogenic GG-dispersion. In this way, a better control over nucleation and growth of the AgNPs could be achieved. Moreover, according to the literature, a method able to couple the nanoparticles synthesis with the preparation of the film-forming dispersion could facilitate the scaling-up of the production of these nanocomposite films at industrial level (Ortega, Giannuzzi, Arce & García, 2017). Despite these considerations, most of the studies concerning the development of nanocomposite films use preformed AgNPs for the scope.

Therefore, initial studies aimed at evaluating the capacity of the PE samples to reduce $Ag^+$ to $Ag^0$ and induce the formation of AgNPs. This investigation was carried out on $AgNO_3$ aqueous solutions at two different concentrations (0.5 and 5.0 mg/mL). The effective reduction of $Ag^+$ and the consequent formation of AgNPs was evaluated by spectrophotometric analysis. Indeed, according to the literature (Fei et al., 2014; Sun et al., 2021), AgNPs show a characteristic peak of surface plasmon resonance at around 460 nm, as shown in Fig. 1A.

The highest concentration (5.0 mg/mL) resulted in the formation of aggregates irrespective from the $AgNO_3$:PE weight ratio tested. On the contrary, it was possible to obtain stable colloidal dispersions of AgNPs with the 0.5 mg/mL $AgNO_3$ solution and using a weight amount of PE exactly corresponding to that of the silver salt in solution (1:1 weight ratio), as shown by the DLS data reported in Fig. 1B (the corresponding mean hydrodynamic diameter and PDI values are reported in Table S2 of the supplementary material). Despite it has been reported that PE can act as a surface stabiliser of AgNPs (Sun et al., 2021), higher amounts of PE did not lead to significant improvements in the mean hydrodynamic diameter and homogeneity of the dispersions. An attempt was made to produce the AgNPs at higher temperature, *i.e.* 80 °C instead of 65 °C, as this parameter could critically affect the physical-chemical properties of the resulting nanoparticles (Nguyen, Dang, Doan & Nguyen, 2023). However, a general worsening of the characteristics of the AgNPs was observed, as reported in Fig. 1C (the corresponding mean hydrodynamic diameter and PDI values are reported in Table S2 of the supplementary material), probably due to partial degradation of the PE sample or to interference in the aggregation of growing AgNPs (Liaqat, Jahan, Khalil-Ur-Rahman, Anwar & Qureshi, 2022).

Therefore, based on these results, AgNPs were let form at 65 °C using 0.5 mg/mL $AgNO_3$ solutions and a 1:1 *w/w* $AgNO_3$:PE ratio. The synthesis of the AgNPs was carried out within the film-forming solutions, which were composed of GG and a plasticising agent. The chemical reduction of $Ag^+$ directly in the film-forming solution should allow a better and more uniform dispersion of AgNPs within the polymeric mixture and, consequently, within the corresponding polymeric film, compared to the use of preformed AgNPs.

Two different plasticising agents, namely Gly and $PEG_{400}$, were combined with GG to allow the formation of polymeric films with adequate mechanical properties, as it is known that low acyl GG forms rigid and brittle films (Paolicelli et al., 2018). PEGs of higher molecular weight were discarded because they caused a significant shift in the sol-gel transition temperature of GG, towards higher temperature values (Fig. 2A). Therefore, their use would have required higher temperatures for the solvent casting procedure, which might degrade the PE components. On the contrary, the presence of the PE did not modify the sol-gel transition temperature of the polymer (Fig. 2B). Furthermore, neither

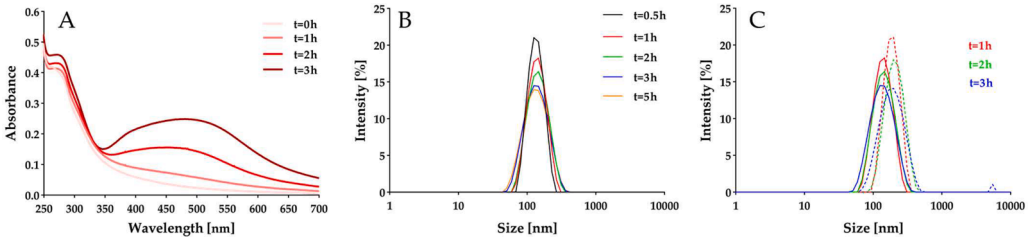


**Fig. 1.** Analysis of solutions of silver nitrate salt in the presence of PE, showing the progressive reduction of $Ag^+$ to $Ag^0$ and subsequent formation of AgNPs: (A) UV–Visible absorbance spectra with a characteristic peak at around 460 nm; (B) and (C) DLS analysis showing the effect of time and temperature on AgNPs formation (65 °C solid lines; 80 °C dashed lines); the corresponding mean hydrodynamic diameter and PDI values are reported in Table S2 of the supplementary material.

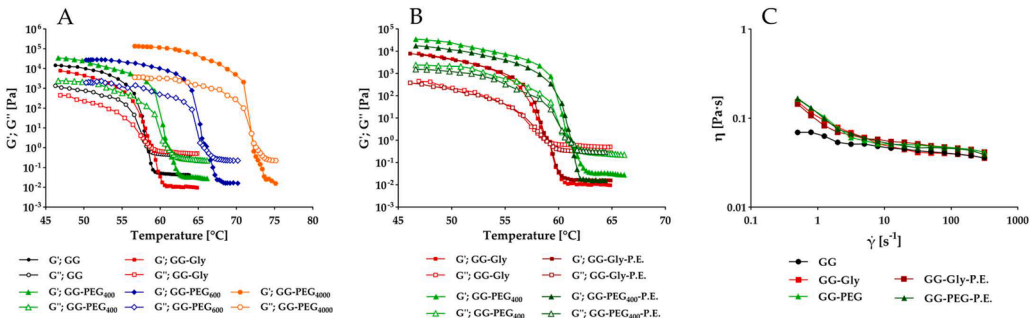


**Fig. 2.** (A) Temperature sweeps showing the effect of different plasticising agents (Gly, $PEG_{400}$, $PEG_{600}$ and $PEG_{4000}$) on the sol-gel transition temperature of GG. (B) Temperature sweeps showing the effect of PE on the sol-gel transition temperature of GG/Gly or GG/$PEG_{400}$ mixtures.

Gly, nor $PEG_{400}$ or PE significantly affected the pseudoplastic behaviour of GG (Fig. 2C), therefore they should not interfere with the casting procedure.

Under these experimental conditions, nanocomposite GG-based films were produced following two different procedures, as reported in Section 2.4. The first method involved the initial formation of the AgNPs and the subsequent addition of solid GG to the colloidal dispersion. However, this procedure did not allow to achieve complete polymer dissolution, probably due to the low temperature set (Fiorica et al., 2021), thus resulting in the formation of F1-Gly and F1-PEG films with poor homogeneity. For this reason, a different procedure was adopted for the preparation of the film-forming mixture, which involved the initial dissolution of GG and the plasticising agent and the subsequent formation of the AgNPs in the presence of the polymer. This procedure allowed to achieve both proper polymer dissolution and *in situ* formation of the AgNPs, as indicated by the digital images reported in Figure S4. Following this method, the AgNPs are produced in the presence of GG, which can assist their formation, as it can form coordination bond with $Ag^+$ ions, thus facilitating their reduction (Biscari et al., 2024). A schematic of the procedure used to prepare all these nanocomposite films is reported in the supplementary material (Figure S3).

Under the optimised conditions homogeneous F2-Gly, F2-PEG, F3-Gly and F3-PEG nanocomposite films were formed, which differ for the silver content. More specifically, F2-Gly and F2-PEG films contain ~0.12 mg/$cm^2$, whereas F3-Gly and F3-PEG films contain ~0.24 mg/$cm^2$. Similar results were reported for starch-based nanocomposite films embedding *in situ* synthesised AgNPs (Ortega, García & Arce, 2019), which, however, have three order of magnitude lower content of AgNPs than the film formulations here reported.

The same experimental conditions, schematised in Figure S3, were also adopted to produce plain films, non-containing AgNPs (F0-Gly and F0-PEG), which were used as a control.

### 3.3. Film characterisation

All the formulations showed uniform thickness, with mean values lower than 85 μm, which allow defining the samples as polymeric thin films. Irrespective from the plasticising agent used, the presence of the AgNPs did not affect the mean thickness of the films, as shown by the results reported in Table 1. On the contrary, both the AgNPs content and the type of plasticising agent used influence the colour characters of the film samples. Data reported in Table S3 show an evident and similar browning for the two used plasticising agents due to $Ag^+$ reduction and AgNPs formation. More specifically, L*, or lightness, values of about 89 in F0-Gly and F0-PEG decrease to about 84 in F2-Gly and F2-PEG films containing AgNPs. L* furtherly decrease to about 80 both in F3-Gly and F3-PEG, in which the silver content was doubled, but from a statistical point of view, the difference respect to the reference, is much more pronounced in the system containing Gly ($\Delta E = 23.33$), in which the yellowness, positive b* value, increases much more. Similar results were already reported with gelatin- and polydimethylsiloxane-based films, where increments in the AgNPs concentration produce an increase in total colour difference (Pérez-Marroquín et al., 2022; Yao, Fostier & Barros Santos, 2020). In our case, the four film samples containing silver show an analogous browning behaviour, even if they acquire different colour, with a more pronounced tonality ($h_{ab}$) difference in PEG-plasticised films and a more pronounced Chroma ($C^*_{ab}$) difference in Gly-plasticised samples. The presence of the AgNPs also produced a slight decrease in the optical transparency of the obtained GG-based films, which resulted more pronounced and statistically significant in PEG-plasticised film samples (Table S3). However, the degree of transparency of F2-PEG and F3-PEG films still results adequate to allow for the monitoring of wound-healing progress without having to replace the dressing (Kuddushi, Shah, Ayranci & Zhang, 2023).

**Table 1**
Thickness, density, tensile properties and WVP of plain and nanocomposite GG-based films. The results are mean values ± SD.

| Sample | Thickness (μm) | Density (g $cm^{-3}$) | Tensile modulus (MPa) | Tensile strength (MPa) | WVP ($\times 10^{-6}$, g $m^{-1}$ $h^{-1}$ $Pa^{-1}$) |
|---|---|---|---|---|---|
| F0-Gly | $77\pm2^{f,i}$ | $1.23\pm0.01^{f,i}$ | $336.63\pm27.57^{a,d}$ | $28.67\pm3.49^{a}$ | $1.23\pm0.07^{f,i}$ |
| F0-PEG | $80\pm2^{f,l}$ | $1.24\pm0.01^{f,l}$ | $911.68\pm194.52^{a,e}$ | $43.69\pm4.96^{a}$ | $1.25\pm0.04^{f,l}$ |
| F2-Gly | $77\pm3^{g,i}$ | $1.26\pm0.03^{g,i}$ | $304.33\pm63.31^{b,d}$ | $21.16\pm1.45^{b}$ | $1.31\pm0.01^{g,i}$ |
| F2-PEG | $83\pm1^{g,l}$ | $1.27\pm0.02^{g,l}$ | $1261.00\pm94.32^{b,e}$ | $44.88\pm3.12^{b}$ | $1.23\pm0.01^{g,l}$ |
| F3-Gly | $85\pm2^{h,i}$ | $1.30\pm0.01^{h,i}$ | $222.48\pm28.48^{c,d}$ | $23.26\pm2.20^{c}$ | $1.25\pm0.06^{h,i}$ |
| F3-PEG | $85\pm3^{h,l}$ | $1.31\pm0.02^{h,l}$ | $1046.60\pm100.44^{c,e}$ | $48.47\pm3.46^{c}$ | $1.33\pm0.02^{h,l}$ |

The same superscript letter in the same column indicates the statistical significance.
$^{a,b,c}$ $p < 0.001$.
$^{d,e}$ $p < 0.05$.
$^{f,g,h,i,l}$ $p > 0.05$.

The presence of the AgNPs slightly increased density and WVP of the nanocomposite GG-based films, even if the results are not statistically significant. Increasing of WVP following addition of AgNPs was already reported for agar and carrageenan films (Roy, Shankar & Rhim, 2019; Shankar & Rhim, 2015). The WVP values of the nanocomposite GG-based films indicate a water vapor transmission rate of around 1800 g/$m^2$ per 24 h, which it has been reported to be adequate to maintain an optimal moisture content for the proliferation and regular function of epidermal cells and fibroblasts, thus promoting the wound healing process (Xu et al., 2016).

Both F0-Gly and F0-PEG films were characterised by SEM and EDS analysis and the related results are shown in Fig. 3.

Both films display carbon and oxygen as the main constituents of the

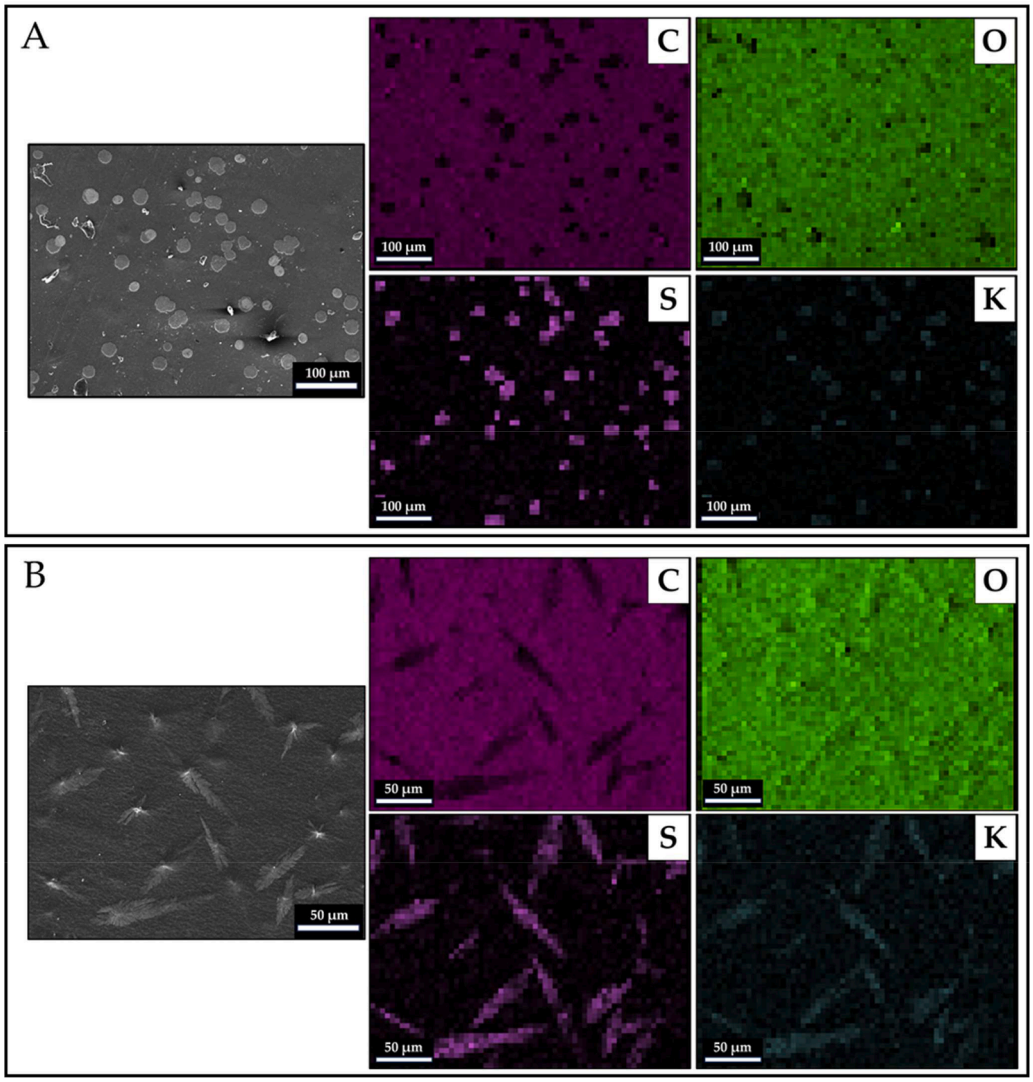


**Fig. 3.** SEM micrographs and related EDS analysis of (A) F0-Gly (1.25kX) and (B) F0-PEG films (2.5kX). (C = carbon, O = oxygen, S = sulfur, K = potassium).

polymeric film, while a significant concentration of sulphur and potassium was detected in the PE, deriving from soil fertilisers (Clark & Smith, 1988; Dutta et al., 2023; Pacheco et al., 2008). It can be observed the presence of some dendritic structures, which can be due to the extract, as suggested by the results of the EDS analysis. Similar results were already observed by Sun et al. (2021). However, despite being characterised by a comparable chemical composition, the PE display a completely different morphology in glycerol-plasticised (F0-Gly) and PEG-plasticised (F0-PEG) films. In particular, F0-Gly are characterised by a flower-like shape, which can be almost equated to a spherical shape where the extracts tend to reduce as much as possible their exposed surface, instead F0-PEG are characterised by a leaf-like shape, which is much more elongated. This difference can be likely ascribed to the different interaction of glycerol over PEG with GG, due to the diverse hydrogen bonding ability, which lead to different tridimensional networks (Domján, Bajdik & Pintye-Hódi, 2009). Similar results were also observed for the F2 and F3 films and Fig. 4 shows the SEM and EDS analysis of both F3-Gly and F3-PEG films.

EDS analysis highlighted that silver is homogeneously dispersed throughout the whole matrix, which evidenced uniform silver content within all the nanocomposite films produced.

The $Ag^{+}$ ions deriving from the $AgNO_3$ salt tends to reduce and cluster to form the $Ag^{0}$ nanoparticles, like the ones shown in Fig. 5.

The different interaction of Gly and PEG with GG was also evidenced by the measurement of the tensile properties of the F0-Gly and F0-PEG films, not containing the AgNPs. F0-PEG films proved to be more performing than F0-Gly ones, with a tensile modulus 170.8 % and a tensile strength 52.4 % higher, which account for a different plasticising ability of Gly over $PEG_{400}$ due to the intrinsic higher molecular weight of PEG.

The advantages of PEG over Gly in terms of tensile properties are confirmed also for the F2 and F3 samples containing the AgNPs, where PEG displays an increase of 2.7 % and 10.9 % in tensile strength, while Gly experiences a decrease of 26.2 % and 21.3 % in this parameter. This difference in behaviour may be likely ascribed to a different disposition of the AgNPs within the polymeric films due to the different interaction of GG with the two plasticisers and their different hydrophilic nature. In particular, the AgNPs act as stress intensifiers rather than as reinforcement in the presence of glycerol, on the contrary, they can act as film reinforcement in the presence of PEG.

Inferential statistic was used to determine if the film type and the Ag content met the criteria for statistical significance proving to have an actual effect on tensile modulus and strength. Results are reported in the supplementary material (Tables S4 and S5). It can be noticed that film type plays the most statistical significant role for both tensile modulus and strength, thus confirming the clear superiority of PEG films over Gly ones. Concerning the interaction between Ag content and film type, it also proved to be statistical significant for both tensile parameters, thus corroborating the hypothesis that increasing Ag content induce a

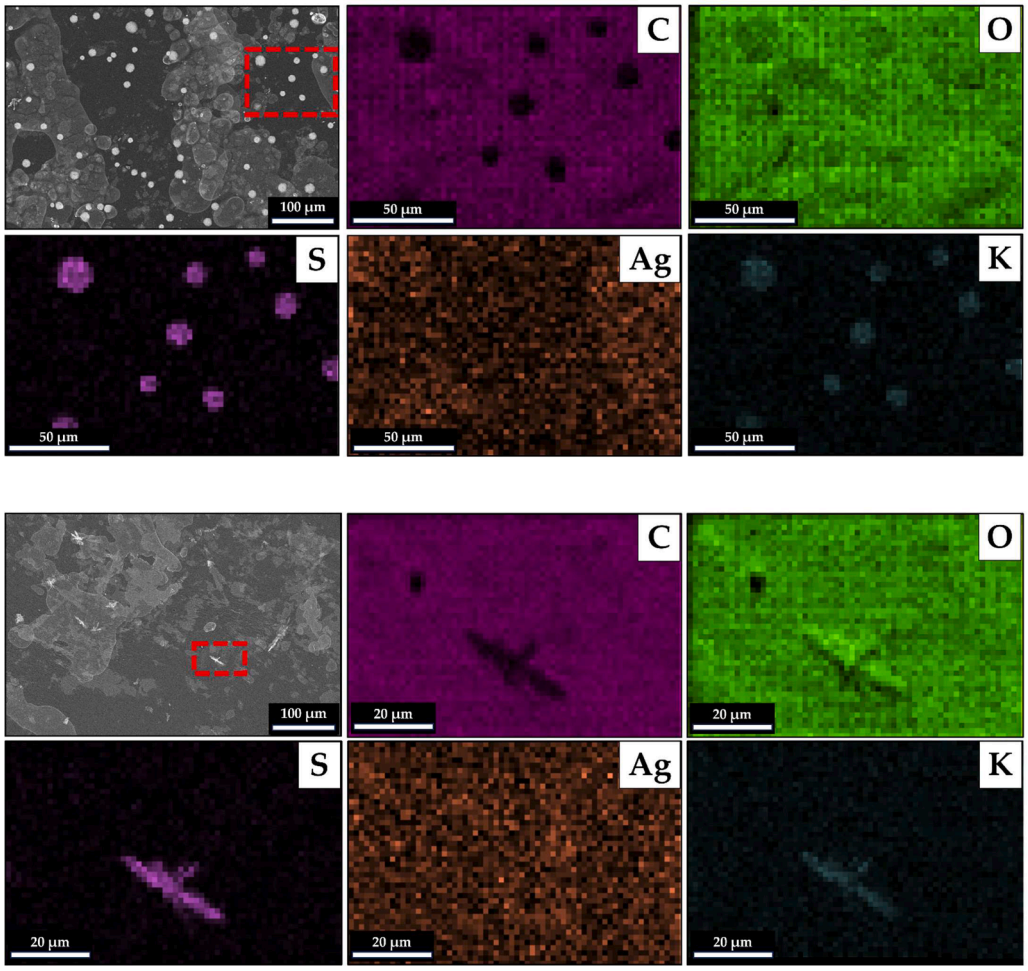


**Fig. 4.** SEM micrographs and related EDS analysis of F3-Gly (1.25kX) and F3-PEG (1.25kX) films. (C = carbon, O = oxygen, S = sulfur, Ag = silver, K = potassium).

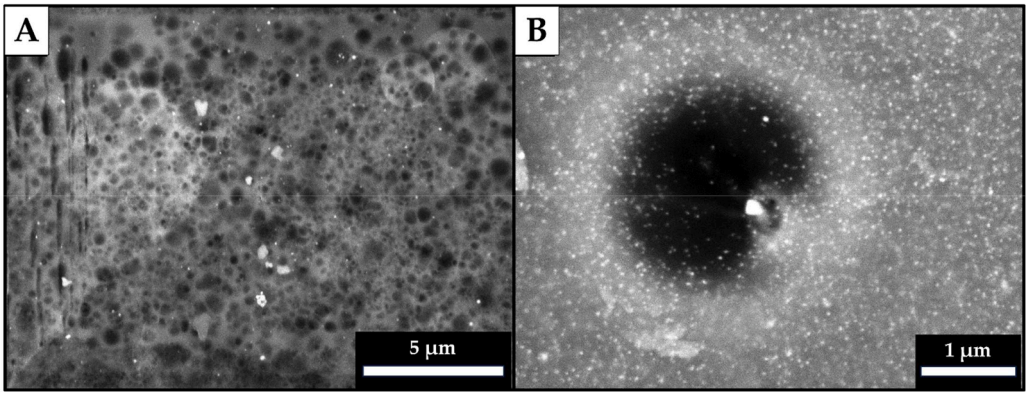


**Fig. 5.** AgNPs in F3-Gly (37.5vkX) (A) and F3-PEG (125vkX) (B) films.

different mechanical response according to the base polymer used to produce the film.

Both these effects have been reported in the literature and, in particular, it has been reported that when NPs are locally agglomerated within a polymer matrix they can act as stress-concentrating centres, thereby decreasing the mechanical strength of the material (Han, Kiat-amnuay, Powers & Zhao, 2008).

### 3.4. Swelling measurements

All F-Gly and F-PEG films were characterised for their ability to swell when in contact with physiological fluids. Swelling studies were performed in both PB (pH = 7.4, $I$ = 0.10) and PBS (pH = 7.4, $I$ = 0.16), which differ for the ionic strength. Results were expressed in terms of Q and are reported in Fig. 6A and B. Both Gly-plasticised and PEG-plasticised formulations show similar swelling behaviour over time, with only marginal difference in the plateau value. In particular, it can be observed an increase in the swelling degree with increasing silver

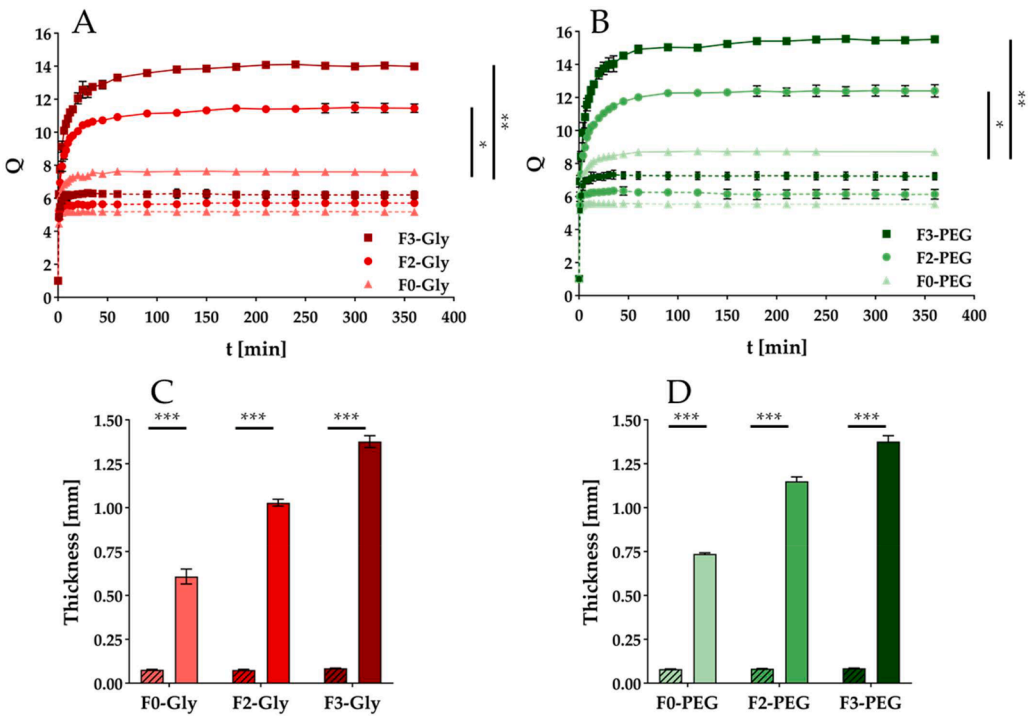


**Fig. 6.** Dynamic swelling capacity measured in PB (solid lines) and PBS (dashed lines) at 37.0 ± 0.1 °C of (A) Gly-plasticised films and (B) PEG-plasticised films. Thickness before and after swelling in PB of (C) Gly-plasticised films and (D) PEG-plasticised films (*$p < 0.01$; ** $p < 0.001$; ***$p < 0.0001$).

content. Indeed, plain films (F0-Gly and F0-PEG) show Q values of around 8, whereas nanocomposite films (F2-Gly, F2-PEG, F3-Gly and F3-PEG) are able to absorb PB increasing over 10 times their weight, as also proven by the significative variation of film thickness, measured at the end of the swelling study in PB (Fig. 6C and D). The same trend is maintained in PBS, even if lower Q values were reached (Fig. 6A and B dashed lines), due to the higher ionic strength of PBS ($I = 0.16$) compared to PB ($I = 0.10$), as also reported for high acyl GG hydrogels (Kanyuck, Mills, Norton & Norton-Welch, 2021). The swelling behaviour makes these nanocomposite films able to absorb wound exudate, while maintaining a moist wound bed, which it has been proven to facilitate the healing process of the wound. Moreover, the similar behaviour observed between Gly-plastisiced and PEG-plasticised nanocomposite films suggest that a similar trend in the release profile of AgNPs can be supposed for the two film formulations, which, therefore, could present similar biological properties.

### 3.5. Antifungal activity of films loaded with AgNPs

In a first set of experiments, we tested the growth of yeast on F0-Gly and F0-PEG without AgNPs on Candida spp. As shown in Table 2, all Candida spp. were able to grow on these films, with no differences with respect to the control.

**Table 2**
Growth on films (F0-Gly and F0-PEG) of Candida spp. expressed as CFU/mL.

| | 24 h | | | 48 h | | |
|---|---|---|---|---|---|---|
| Candida spp | Control | F0-Gly | F0-PEG | Control | F0-Gly | F0-PEG |
| *C. albicans* | $1.3 \times 10^5$ | $1.4 \times 10^5$ | $1.5 \times 10^5$ | $1 \times 10^6$ | $1 \times 10^6$ | $1 \times 10^6$ |
| *C. lusitaniae* | $1 \times 10^6$ | $1 \times 10^6$ | $1 \times 10^6$ | $1 \times 10^6$ | $1 \times 10^6$ | $1 \times 10^6$ |
| *C. haemulonii* | $1 \times 10^6$ | $3.5 \times 10^4$ | $2.2 \times 10^4$ | $1 \times 10^6$ | $1 \times 10^6$ | $1 \times 10^6$ |
| *C. krusei* | $1 \times 10^6$ | $1 \times 10^6$ | $1 \times 10^6$ | $1 \times 10^6$ | $1 \times 10^6$ | $1 \times 10^6$ |
| *C. glabrata* | $1 \times 10^5$ | $1 \times 10^6$ | $2.6 \times 10^5$ | $1 \times 10^5$ | $1 \times 10^6$ | $1 \times 10^6$ |

CFU = Colony forming units.

The antifungal activity of the AgNPs contained in F2-Gly or F2-PEG was tested on five Candida species, namely *C. albicans, C. haemulonii, C. lusitaniae, C. krusei* and *C. glabrata*. Fig. 7 shows the histograms of the results obtained for each species. The results were expressed as Colony Forming Units per millilitre (CFU/mL) after 24 or 48 h of growth in the presence of the films. It should be noted that all the species studied are sensitive to the AgNPs after 24 or 48 h of contact with F2-Gly and F2-PEG formulations. In particular, in the first 24 h of growth, the number of CFUs was reduced in all species, with $p < 0.0001$ in *C. albicans, C. lusitaniae* and *C. glabrata*, and $p < 0.05$ in other species. No differences were found between F2-Gly and F2-PEG at concentration of 0.063 mg/mL of AgNPs. After 48 h of growth, all species tested were inhibited in the presence of films with $p < 0.0001$.

In another set of experiments, the antifungal activity of F3-Gly and F3-PEG with 0.126 mg/mL of AgNPs was performed on Candida spp. (Fig. 8). All Candida spp. tested confirmed the previous results. All species are inhibited in the presence of F3-Gly and F3-PEG. Therefore, the minimum required concentration of silver to inhibit the growth of all fungal species is 0.063 mg/mL AgNPs. Similar results were reported by other authors (Cho, Kim, Kim, Park & Lee, 2019) where Ag-PPFC (plasma polymer fluorocarbon) nanocomposite thin films were found to have superior antimicrobial properties, suppressing the growth and proliferation of bacteria by up 92.2 % compared with uncoated substrates. Therefore, combining traditional medicine with nanotechnology opens the door to innovative strategies for treating skin and soft tissue infections and also contributes to the fight against the rise of antimicrobial resistance (Mussin et al., 2021).

## 4. Conclusions

This work demonstrates the feasibility of developing nanocomposite GG-based films embedding AgNPs with a one-step procedure, using a polyphenol-rich extract obtained from kiwi peels for the bioreduction of

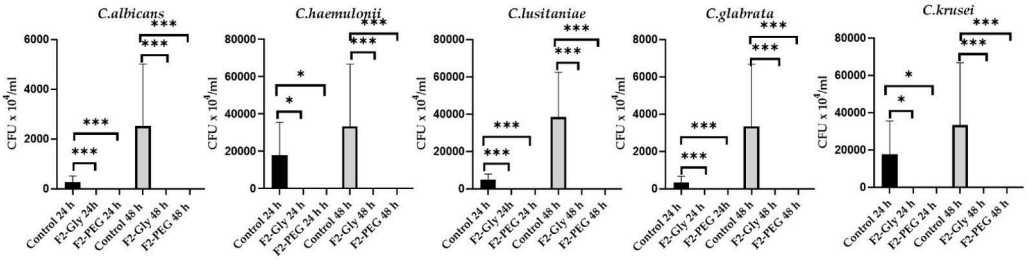


**Fig. 7.** Antifungal activity of film F2- Gly and F2-PEG against Candida spp after 24 h and 48 h of growth (* $p < 0.05$; ***$p < 0.0001$).

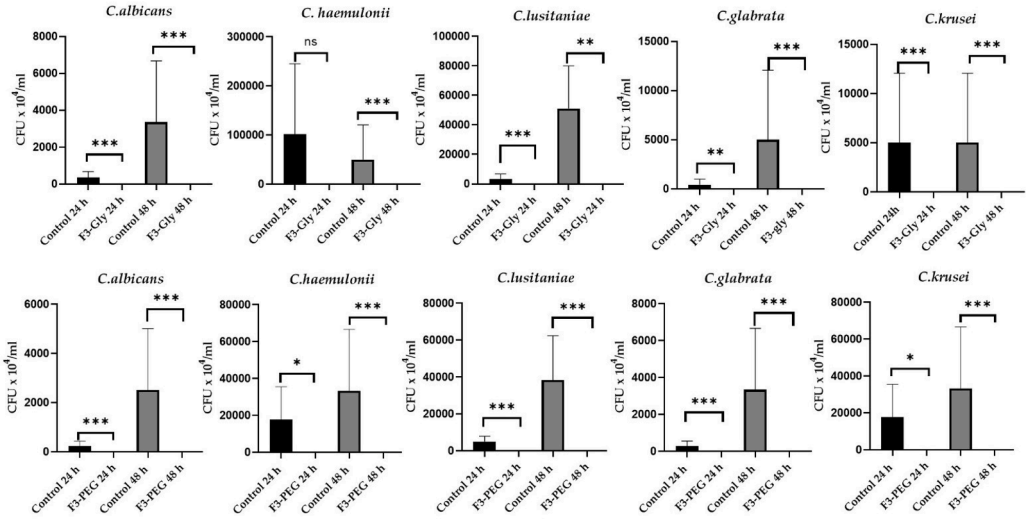


**Fig. 8.** Antifungal activity of F3-Gly and F3-PEG against Candida spp. after 24 h and 48 h of growth (* $p < 0.05$; ***$p < 0.0001$).

a silver salt. The optimised procedure allowed the formation of AgNPs directly within the film-forming solutions, which were formed by low acyl gellan gum and a plasticising agent. The presence of the AgNPs did not interfere with the casting procedure, whereas their distribution within the final film sample was influenced by the specific plasticising agent used. This feature had consequences on the tensile behaviour of the films. If nanocomposite films plasticised with Gly showed a slight worsening of the mechanical properties, those prepared with $PEG_{400}$, as the plasticising agent, showed a certain increase in the tensile strength and tensile modulus in the presence of AgNPs. Nevertheless, both Gly-plasticised and $PEG_{400}$-plasticised films showed similar antifungal activity. Therefore, considering that both GG-Gly and GG-PEG films containing AgNPs displayed an effective antifungal activity, their tensile behaviour proved to be determinant in identifying the best solution for wound dressing.

Globally, the present study provides a green approach to develop nanocomposite thin films, containing AgNPs obtained by reduction of silver salts mediated by natural extracts. In particular, it offers an approach that deserves consideration, for the recycling and valorisation of biomolecules recovered from the wastes of agri-food industry. The nanocomposite films obtained following this method can be proposed for wound dressing or even food packaging, to prevent microbial and yeast contaminations. In this sense, further investigations are needed to confirm the effectiveness of the developed nanocomposite films under different conditions of use and to evaluate their stability and effectiveness over time.

## Funding

"This research received no external funding".

## CRediT authorship contribution statement

**Laura Di Muzio:** Writing – review & editing, Visualization, Validation, Methodology, Investigation, Formal analysis, Data curation, Conceptualization. **Francesco Cairone:** Writing – review & editing, Validation, Methodology, Investigation, Formal analysis, Data curation. **Stefania Cesa:** Writing – review & editing, Supervision, Resources. **Claudia Sergi:** Writing – review & editing, Visualization, Validation, Methodology, Investigation, Formal analysis, Data curation. **Jacopo Tirillò:** Supervision, Resources. **Letizia Angiolella:** Writing – review & editing, Visualization, Validation, Resources, Methodology, Formal analysis, Data curation. **Andrea Giammarino:** Investigation. **Gustavo Giusiano:** Investigation, Writing – review & editing. **Stefania Petralito:** Writing – review & editing, Supervision. **Maria Antonietta Casadei:** Writing – review & editing, Supervision, Resources. **Patrizia Paolicelli:** Writing – review & editing, Writing – original draft, Validation, Supervision, Resources, Project administration, Methodology, Formal analysis, Data curation, Conceptualization.

## Declaration of competing interest

The authors declare that they have no known competing financial interests or personal relationships that could have appeared to influence the work reported in this paper.

## Data availability

The data presented in this study are available on request to the corresponding authors.

## Supplementary materials

Supplementary material associated with this article can be found, in the online version, at doi:10.1016/j.carpta.2024.100485.

## References


Adrover, A., Di Muzio, L., Trilli, J., Brandelli, C., Paolicelli, P., Petralito, S., & Casadei, M. A. (2020). Enhanced loading efficiency and mucoadhesion properties of Gellan Gum thin films by complexation with hydroxypropyl-β-cyclodextrin. *Pharmaceutics, 12*(9), 819. https://doi.org/10.3390/pharmaceutics12090819

Ahamad, I., Bano, F., Anwer, R., Srivastava, P., Kumar, R., & Fatma, T. (2022). Antibiofilm activities of biogenic silver nanoparticles against *Candida albicans*. *Frontiers in Microbiology, 12*, Article 741493. https://doi.org/10.3389/fmicb.2021.741493

Aires, A., & Carvalho, R. (2020). Kiwi fruit residues from industry processing: Study for a maximum phenolic recovery yield. *Journal of Food Science and Technology, 57*(11), 4265–4276. https://doi.org/10.1007/s13197-020-04466-7

AlJindan, R., & AlEraky, D. M. (2022). Silver nanoparticles: A promising antifungal agent against the growth and biofilm formation of the emergent *Candida auris*. *Journal of Fungi (Basel), 8*(7), 744. https://doi.org/10.3390/jof8070744

Bharathi, D., Lee, J., Karthiga, P., Mythili, R., Devanesan, S., & AlSalhi, M. S. (2023). Kiwi fruit peel biowaste mediated green synthesis of silver nanoparticles for enhanced dye degradation and antibacterial activity. *Waste & Biomass Valorization*. https://doi.org/10.1007/s12649-023-02328-9

Biscari, G., Malkoch, M., Fiorica, C., Fan, Y., Palumbo, F. S., Indelicato, S., Bongiorno, D., & Pitarresi, G. (2024). Gellan gum-dopamine mediated in situ synthesis of silver nanoparticles and development of nano/micro-composite injectable hydrogel with antimicrobial activity. *International Journal of Biological Macromolecules, 258*, Article 128766. https://doi.org/10.1016/j.ijbiomac.2023.128766

Cairone, F., Garzoli, S., Menghini, L., Simonetti, G., Casadei, M. A., Di Muzio, L., & Cesa, S. (2022). Valorization of kiwi peels: Fractionation, bioactives analyses and hypotheses on complete peels recycle. *Foods (Basel, Switzerland), 11*(4), 589. https://doi.org/10.3390/foods11040589

Cairone, F., Petralito, S., Scipione, L., & Cesa, S. (2021). Study on extra virgin olive oil: Quality evaluation by anti-radical activity, color analysis, and polyphenolic HPLC-DAD analysis. *Foods (Basel, Switzerland), 10*(8), 1808. https://doi.org/10.3390/foods10081808

Cairone, F., Salvitti, C., Iazzetti, A., Fabrizi, G., Troiani, A., Pepi, F., & Cesa, S. (2023). In-depth chemical characterization of *Punica granatum* L. Seed Oil. *Foods (Basel, Switzerland), 12*(8), 1592. https://doi.org/10.3390/foods12081592

Chamorro, F., Carpena, M., Fraga-Corral, M., Echave, J., Riaz Rajoka, M. S., Barba, F. J., Cao, H., Xiao, J., Prieto, M. A., & Simal-Gandara, J (2022). Valorization of kiwi agricultural waste and industry by-products by recovering bioactive compounds and applications as food additives: A circular economy model. *Food Chemistry, 370*, Article 131315. https://doi.org/10.1016/j.foodchem.2021.131315

Chen, X., Li, H., Qiao, X., Jiang, T., Fu, X., He, Y., & Zhao, X. (2021). Agarose oligosaccharide-silver nanoparticle-antimicrobial peptide-composite for wound dressing. *Carbohydrate Polymers, 269*, Article 118258. https://doi.org/10.1016/j.carbpol.2021.118258

Cho, E., Kim, S. H., Kim, M., Park, J. S., & Lee, S. J. (2019). Super-hydrophobic and antimicrobial properties of Ag-PPFC nanocomposite thin films fabricated using a ternary carbon nanotube-Ag-PTFE composite sputtering target. *Surface & Coatings Technology, 370*, 18–23. https://doi.org/10.1016/j.surfcoat.2019.04.045

Clark, C. J., & Smith, G. S. (1988). Seasonal accumulation of mineral nutrients by kiwifruit 2. Fruit. *New Phytologist, 108*, 399–409. https://doi.org/10.1111/j.1469-8137.1988.tb04180.x

Deng, J., Liu, Q., Zhang, C., Cao, W., Fan, D., & Yang, H. (2016). Extraction optimization of polyphenols from waste kiwi fruit seeds (*Actinidia chinensis* Planch.) and evaluation of its antioxidant and anti-inflammatory properties. *Molecules (Basel, Switzerland), 21*(7), 832. https://doi.org/10.3390/molecules21070832

Di Muzio, L., Simonetti, P., Carriero, V. C., Brandelli, C., Trilli, J., Sergi, C., Tirillò, J., Cairone, F., Cesa, S., Radocchia, G., Schippa, S., Petralito, S., Paolicelli, P., & Casadei, M. A. (2022). Solvent casting and UV photocuring for easy and safe fabrication of nanocomposite film dressings. *Molecules (Basel, Switzerland), 27*(9), 2959. https://doi.org/10.3390/molecules27092959

Dias, M., Caleja, C., Pereira, C., Calhelha, R. C., Kostic, M., Sokovic, M., Tavares, D., Baraldi, I. J., Barros, L, & Ferreira, I. C. (2020). Chemical composition and bioactive properties of byproducts from two different kiwi varieties. *Food Research International, 127*, Article 108753. https://doi.org/10.1016/j.foodres.2019.108753

Domján, A., Bajdik, J., & Pintye-Hódi, K. (2009). Understanding of the plasticizing effects of glycerol and PEG 400 on chitosan films using solid-state NMR spectroscopy. *Macromolecules, 42*(13), 4667–4673. https://doi.org/10.1021/ma8021234

Dutta, S. K., Layek, J., Yadav, A., Das, S. K., Rymbai, H., Mandal, S., Sahana, N., Bhutia, T. L., Devi, E. L., Patel, V. B., Laha, R., & Mishra, V. K. (2023). Improvement of rooting and growth in kiwifruit (*Actinidia deliciosa*) cuttings with organic biostimulants. *Heliyon, 9*(7), e17815. https://doi.org/10.1016/j.heliyon.2023.e17815

Fei, J., Zhao, J., Du, C., Wang, A., Zhang, H., Dai, L., & Li, J. (2014). One-pot ultrafast self-assembly of autofluorescent polyphenol-based core@shell nanostructures and their selective antibacterial applications. *ACS Nano, 8*(8), 8529–8536. https://doi.org/10.1021/nn504077c

Fiorica, C., Biscari, G., Palumbo, F. S., Pitarresi, G., Martorana, A., & Giammona, G. (2021). Physicochemical and rheological characterization of different low molecular weight gellan gum products and derived ionotropic crosslinked hydrogels. *Gels, 7*(2), 62. https://doi.org/10.3390/gels7020062

Gabaldón, T., Naranjo-Ortíz, M. A., & Marcet-Houben, M. (2016). Evolutionary genomics of yeast pathogens in the Saccharomycotina. *FEMS Yeast Research, 16*, fow064. https://doi.org/10.1093/femsyr/fow064

Gibała, A., Żeliszewska, P., Gosiewski, T., Krawczyk, A., Duraczyńska, D., Szaleniec, J., Szaleniec, M., & Oćwieja, M. (2021). Antibacterial and antifungal properties of silver nanoparticles-effect of a surface-stabilizing agent. *Biomolecules, 11*(10), 1481. https://doi.org/10.3390/biom11101481

Gil-Martín, E., Forbes-Hernández, T., Romero, A., Cianciosi, D., Giampieri, F., & Battino, M. (2022). Influence of the extraction method on the recovery of bioactive phenolic compounds from food industry by-products. *Food Chemistry, 378*, Article 131918. https://doi.org/10.1016/j.foodchem.2021.131918

Hădărugă, D. I., Pantea, C., & Hădărugă, N. G. (2016). Antioxidant activity and kinetics on kiwi fruit (*Actinidia deliciosa*) ethanolic extracts by 2, 2-diphenyl-1-picrylhydrazyl (DPPH·) method. *Journal of Agroalimentary Process and Technologies, 22*, 207–211.

Han, Y., Kiat-amnuay, S., Powers, J. M., & Zhao, Y. (2008). Effect of nano-oxide concentration on the mechanical properties of a maxillofacial silicone elastomer. *The Journal of Prosthetic Dentistry, 100*(6), 465–473. https://doi.org/10.1016/S0022-3913(08)60266-8

Huang, K., Maltais, A., & Wang, Y. (2023). Enhancing water resistance of regenerated cellulose films with organosilanes and cellulose nanocrystals for food packaging. *Carbohydrate Polymer Technologies and Applications, 6*, Article 100391. https://doi.org/10.1016/j.carpta.2023.100391

Kainz, K., Bauer, M. A., Madeo, F., & Carmona-Gutierrez, D. (2020). Fungal infections in humans: The silent crisis. *Microbial Cell, 7*(6), 143–145. https://doi.org/10.15698/mic2020.06.718

Kanniah, P., Chelliah, P., Thangapandi, J. R., Gnanadhas, G., Mahendran, V., & Robert, M. (2021). Green synthesis of antibacterial and cytotoxic silver nanoparticles by *Piper nigrum* seed extract and development of antibacterial silver based chitosan nanocomposite. *International Journal of Biological Macromolecules, 189*, 18–33. https://doi.org/10.1016/j.ijbiomac.2021.08.056

Kanyuck, K. M., Mills, T. B., Norton, I. T., & Norton-Welch, A. B. (2021). Swelling of high acyl gellan gum hydrogel: Characterization of network strengthening and slower release. *Carbohydrate Polymers, 259*, Article 117758. https://doi.org/10.1016/j.carbpol.2021.117758

Khansa, I., Schoenbrunner, A. R., Kraft, C. T., & Janis, J. E. (2019). Silver in wound care-friend or foe?: A comprehensive review. *Plastic and Reconstructive Surgery. Global Open, 7*(8), e2390. https://doi.org/10.1097/gox.0000000000002390

Kuddushi, M., Shah, A. A., Ayranci, C., & Zhang, X. (2023). Recent advances in novel materials and techniques for developing transparent wound dressings. *Journal of Materials Chemistry B, 11*(27), 6201–6224. https://doi.org/10.1039/d3tb00639e

Liaqat, N., Jahan, N., Khalil-Ur-Rahman, Anwar, T., & Qureshi, H. (2022). Green synthesized silver nanoparticles: Optimization, characterization, antimicrobial activity, and cytotoxicity study by hemolysis assay. *Frontiers in Chemistry, 10*, Article 952006. https://doi.org/10.3389/fchem.2022.952006

Liu, Z., Shi, L., Qi, Y., Barrow, C. J., Dunshea, F. R., & Suleria, H. A. (2022). Antioxidative properties and phenolic profile of the core, pulp and peel of commercialized kiwifruit by LC-ESI-QTOF-MS/MS. *Processes, 10*(9), 1811. https://doi.org/10.3390/pr10091811

Malik, M. A., Batterjee, M. G., Kamli, M. R., Alzahrani, K. A., Danish, E. Y., & Nabi, A. (2022). Polyphenol-capped biogenic synthesis of noble metallic silver nanoparticles for antifungal activity against *Candida auris*. *Journal of Fungi (Basel), 8*(6), 639. https://doi.org/10.3390/jof8060639

Mogensen, K. B., & Kneipp, K. (2014). Size-dependent shifts of plasmon resonance in silver nanoparticle films using controlled dissolution: Monitoring the onset of surface screening effect. *The Journal of Physical Chemistry C, 118*(48), 28075–28083. https://doi.org/10.1021/jp505632n

Mukherji, S., Bharti, S., Shukla, G., & Mukherji, S. (2019). Synthesis and characterization of size- and shape-controlled silver nanoparticles. *Physical Sciences Reviews, 4*(1), Article 20170082. https://doi.org/10.1515/psr-2017-0082

Mussin, J., Robles-Botero, V., Casañas-Pimentel, R., Rojas, F., Angiolella, L., San Martín-Martínez, E., & Giusiano, G. (2021). Antimicrobial and cytotoxic activity of green synthesis silver nanoparticles targeting skin and soft tissue infectious agents. *Scientific Reports, 11*, 14566. https://doi.org/10.1038/s41598-021-94012-y

Nguyen, N. P. U., Dang, N. T., Doan, L., & Nguyen, T. T. H. (2023). Synthesis of silver nanoparticles: From conventional to 'modern' methods—A review. *Processes, 11*(9), 2617. https://doi.org/10.3390/pr11092617

Nie, P., Zhao, Y., & Xu, H. (2023). Synthesis, applications, toxicity and toxicity mechanisms of silver nanoparticles: A review. *Ecotoxicology and Environmental Safety, 253*, Article 114636. https://doi.org/10.1016/j.ecoenv.2023.114636

Onitsuka, S., Hamada, T., & Okamura, H. (2019). Preparation of antimicrobial gold and silver nanoparticles from tea leaf extracts. *Colloids and Surfaces, 173*, 242–248. https://doi.org/10.1016/j.colsurfb.2018.09.055

Ortega, F., García, M. A., & Arce, V. B. (2019). Nanocomposite films with silver nanoparticles synthesized in situ: Effect of corn starch content. *Food Hydrocolloids, 97*, Article 105200. https://doi.org/10.1016/j.foodhyd.2019.105200

Ortega, F., Giannuzzi, L., Arce, V. B., & García, M. A. (2017). Active composite starch films containing green synthetized silver nanoparticles. *Food Hydrocolloids, 70*, 152–162. https://doi.org/10.1016/j.foodhyd.2017.03.036

Pacheco, C., Calouro, F., Vieira, S., Santos, F., Neves, N., Curado, F., Franco, J., Rodrigues, S., & Antunes, D. (2008). Influence of nitrogen and potassium on yield, fruit quality and mineral composition of kiwifruit. *International Journal of Energy and Environmental Engineering, 1*(2), 9–15.

Paladini, F., & Pollini, M. (2019). Antimicrobial silver nanoparticles for wound healing application: Progress and future trends. *Materials, 12*(16), 2540. https://doi.org/10.3390/ma12162540

Paolicelli, P., Petralito, S., Varani, G., Nardoni, M., Pacelli, S., Di Muzio, L., Tirillò, J., Bartuli, C., Cesa, S., & Casadei, M. A. (2018). Effect of glycerol on the physical and mechanical properties of thin gellan gum films for oral drug delivery. *International Journal of Pharmaceutics, 547*, 226–234. https://doi.org/10.1016/j.ijpharm.2018.05.046

Pérez-Marroquín, X. A., Aguirre-Cruz, G., Campos-Lozada, G., Callejas-Quijada, G., León-López, A., Campos-Montiel, R. G., García-Hernández, L., Méndez-Albores, A., Vázquez-Durán, A., & Aguirre-Álvarez, G. (2022). Green synthesis of silver nanoparticles for preparation of gelatin films with antimicrobial activity. *Polymers, 14*, 3453. https://doi.org/10.3390/polym14173453

Perween, N., Khan, H. M., & Fatima, N. (2019). Silver nanoparticles: An upcoming therapeutic agent for the resistant Candida infections. *Journal of Microbiology & Experimentation, 7*(1), 49–54. https://doi.org/10.15406/jmen.2019.07.00240

Pfaller, M. A., Diekema, D. J., Turnidge, J. D., Castanheira, M., & Jones, R. N. (2019). Twenty years of the SENTRY antifungal surveillance program: Results for Candida species from 1997-2016. *Open Forum Infectious Diseases, 6*(1), S79–S94. https://doi.org/10.1093/ofid/ofy358

Priya, S., Choudhari, M., Tomar, Y., Desai, V. M., Innani, S., Dubey, S. K., & Singhvi, G. (2024). Exploring polysaccharide-based bio-adhesive topical film as a potential platform for wound dressing application: A review. *Carbohydrate Polymers, 327*, Article 121655. https://doi.org/10.1016/j.carbpol.2023.121655

Rahimi, M., Noruzi, E. B., Sheykhsaran, E., Ebadi, B., Kariminezhad, Z., Molaparast, M., Mehrabani, M. G., Mehramouz, B., Yousefi, M., Ahmadi, R., Yousefi, B., Ganbarov, K., Kamounah, F. S., Shafiei-Irannejad, V., & Kafil, H. S. (2020). Carbohydrate polymer-based silver nanocomposites: Recent progress in the antimicrobial wound dressings. *Carbohydrate Polymers, 231*, Article 115696. https://doi.org/10.1016/j.carbpol.2019.115696

Reguengo, L. M., Salgaço, M. K., Sivieri, K., & Marostica Júnior, M. R. (2022). Agro-industrial by-products: Valuable sources of bioactive compounds. *Food Research International, 152*, Article 110871. https://doi.org/10.1016/j.foodres.2021.110871

Rodríguez-Félix, F., López-Cota, A. G., Moreno-Vásquez, M. J., Graciano-Verdugo, A. Z., Quintero-Reyes, I. E., Del-Toro-Sánchez, C. L., & Tapia-Hernández, J. A. (2021). Sustainable-green synthesis of silver nanoparticles using safflower (*Carthamus tinctorius* L.) waste extract and its antibacterial activity. *Heliyon, 7*(4), e06923. https://doi.org/10.1016/j.heliyon.2021.e06923

Rolim, W. R., Pelegrino, M. T., de Araújo Lima, B., Ferraz, L. S., Costa, F. N., Bernardes, J. S., Rodigues, T., Brocchi, M., & Seabra, A. B. (2019). Green tea extract mediated biogenic synthesis of silver nanoparticles: Characterization, cytotoxicity evaluation and antibacterial activity. *Applied Surface Science, 463*, 66–74. https://doi.org/10.1016/j.apsusc.2018.08.203

Roy, S., Shankar, S., & Rhim, J. W. (2019). Melanin-mediated synthesis of silver nanoparticle and its use for the preparation of carrageenan-based antibacterial films. *Food Hydrocolloids, 88*, 237–246.

Salayová, A., Bedlovičová, Z., Daneu, N., Baláž, M., Bujňáková, Z. L., Balážová, L., & Tkáčiková, L. (2021). Green synthesis of silver nanoparticles with antibacterial activity using various medicinal plant extracts: Morphology and antibacterial efficacy. *Nanomaterials, 11*(4), 1005. https://doi.org/10.3390/nano11041005

Shankar, S., & Rhim, J. W. (2015). Amino acid mediated synthesis of silver nanoparticles and preparation of antimicrobial agar/silver nanoparticles composite films. *Carbohydrate Polymers, 130*, 353–363.

Sheokand, B., Vats, M., Kumar, A., Srivastava, C. M., Bahadur, I., & Pathak, S. R. (2023). Natural polymers used in the dressing materials for wound healing: Past, present and future. *Journal of Polymer Science, 61*, 1389. https://doi.org/10.1002/pol.20220734

Silva, S. S., Justi, M., Chagnoleau, J. B., Papaiconomou, N., Fernandez, X., Santos, S. A., Passos, H., Ferreira, A. M., & Coutinho, J. A. (2023). Using biobased solvents for the extraction of phenolic compounds from kiwifruit industry waste. *Separation and Purification Technology, 304*, Article 122344. https://doi.org/10.1016/j.seppur.2022.122344

Stagos, D. (2019). Antioxidant activity of polyphenolic plant extracts. *Antioxidants (Basel), 9*(1), 19. https://doi.org/10.3390/antiox9010019

Sun, X., Zhang, H., Wang, J., Dong, M., Jia, P., Bu, T., Wang, Q., & Wang, L. (2021). Sodium alginate-based nanocomposite films with strong antioxidant and antibacterial properties enhanced by polyphenol-rich kiwi peel extracts bio-reduced silver nanoparticles. *Food Packaging and Shelf Life, 29*, Article 100741. https://doi.org/10.1016/j.fpsl.2021.100741

Tyagi, P. K., Tyagi, S., Gola, D., Arya, A., Ayatollahi, S. A., Alshehri, M. M., & Sharifi-Rad, J. (2021). Ascorbic acid and polyphenols mediated green synthesis of silver nanoparticles from *Tagetes erecta* L. aqueous leaf extract and studied their antioxidant properties. *Journal of Nanomaterials, 2021*, Article 6515419. https://doi.org/10.1155/2021/6515419

Vanlalveni, C., Lallianrawna, S., Biswas, A., Selvaraj, M., Changmai, B., & Rokhum, S. L. (2021). Green synthesis of silver nanoparticles using plant extracts and their antimicrobial activities: A review of recent literature. *RSC Advances, 11*(5), 2804–2837. https://doi.org/10.1039/d0ra09941d

Vazquez-Munoz, R., Lopez, F. D., & Lopez-Ribot, J. L. (2020). Silver nanoantibiotics display strong antifungal activity against the emergent multidrug-resistant yeast *Candida auris* under both planktonic and biofilm growing conditions. *Frontiers in Microbiology, 11*, 1673. https://doi.org/10.3389/fmicb.2020.01673

Xu, R., Xia, H., He, W., Li, Z., Zhano, J., Liu, B., Wang, Y., Lei, Q., Kong, Y., Bai, Y., Yao, Z., Yan, R., Li, H., Zhan, R., Yang, S., Luo, G., & Wu, J. (2016). Controlled water vapor transmission rate promotes wound-healing via wound re-epithelialization and contraction enhancement. *Scientific Reports, 6*, 24596. https://doi.org/10.1038/srep24596

Yao, J. Y., Fostier, A. H., & Barros Santos, E. (2020). In situ formation of gold and silver nanoparticles on uniform PDMS films and colorimetric analysis of their plasmonic color. *Colloids and Surfaces A: Physicochemical and Engineering, 607*, Article 125463. https://doi.org/10.1016/j.colsurfa.2020.125463

Zhang, J., Gao, N., Shu, C., Cheng, S., Sun, X., Liu, C., Xin, G., Li, B., & Tian, J. (2021). Phenolics profile and antioxidant activity analysis of kiwi berry (*Actinidia arguta*) flesh and peel extracts from four regions in China. *Frontiers in Plant Science, 12*, Article 689038. https://doi.org/10.3389/fpls.2021.689038

Zuhrotun, A., Oktaviani, D. J., & Hasanah, A. N. (2023). Biosynthesis of gold and silver nanoparticles using phytochemical compounds. *Molecules (Basel, Switzerland), 28*, 3240. https://doi.org/10.3390/molecules28073240